Journal of Biomedical Optics 9(6), 1244–1252 (November/December 2004)

Optimizing low-light microscopy with back-illuminated electron multiplying charge-coupled device: enhanced sensitivity, speed, and resolution

Colin G. Coates
Donal J. Denvir
Andor Technology Limited
9 Millennium Way
Springvale Business Park, Belfast, BT12 7AL
Northern Ireland

Noel G. McHale
Keith D. Thornbury
Mark A. Hollywood
Queen's University of Belfast
Medical Biology Centre
Smooth Muscle Group
Belfast BT9 7BL
Northern Ireland

Abstract. The back-illuminated electron multiplying charge-coupled device (EMCCD) camera is having a profound influence on the field of low-light dynamic cellular microscopy, combining highest possible photon collection efficiency with the ability to virtually eliminate the readout noise detection limit. We report here the use of this camera, in 512×512 frame-transfer chip format at 10-MHz pixel readout speed, in optimizing a demanding ultra-low-light intracellular calcium flux microscopy setup. The arrangement employed includes a spinning confocal Nipkow disk, which, while facilitating the need to both generate images at very rapid frame rates and minimize background photons, yields very weak signals. The challenge for the camera lies not just in detecting as many of these scarce photons as possible, but also in operating at a frame rate that meets the temporal resolution requirements of many low-light microscopy approaches, a particular demand of smooth muscle calcium flux microscopy. Results presented illustrate both the significant sensitivity improvement offered by this technology over the previous standard in ultra-low-light CCD detection, the GenIII+intensified charge-coupled device (ICCD), and also portray the advanced temporal and spatial resolution capabilities of the EMCCD.
[DOI: 10.1117/1.1805559]

Keywords: charge-coupled device; electron multiplying charge-coupled device; intensified charge-coupled device; calcium flux microscopy; intracellular ion signalling; back-illuminated charge-coupled device; single photon sensitivity; single molecule detection; quantum efficiency; impact ionization.

Paper 03138 received Nov. 24, 2003; revised manuscript received Apr. 13, 2004; accepted for publication Apr. 21, 2004.

1 Introduction

Intracellular ion signalling microscopy (e.g., Ca^{2+} flux microscopy) imposes substantial demands on detector technology, which can fundamentally be filtered down to two key requirements—sensitivity and speed. The detector must be sensitive to: 1. detect the weak signal of low dye concentrations; 2. cope with the lower photon fluxes afforded by shorter exposure times (complementing fast frame rates); 3. detect the weaker photon fluxes afforded by reduced excitation powers (reducing photobleaching of dyes and photodamage to tissues, thereby lengthening experimental lifetimes); and 4. overcome the significant readout noise detection limit of high-speed readout rate. High frame rates are required to facilitate the recording of fast calcium flux processes, in accordance with the major temporal resolution requirements of intracellular ion signalling studies. Ca^{2+} sparks have been recorded in a variety of cell types, including smooth muscle cells.[1–5] These events represent the spontaneous release of Ca^{2+} from ryanodine sensitive intracellular stores, and are characterized by their rapid rise time (20 to 95 ms), decay (27 to 60 ms), and limited spatial spread ($<2\ \mu m^2$).[2] Currently available imaging systems can record spark activity in whole cells, but few are capable of delivering frame rates in excess of 30 fps, particularly while maintaining good resolution in terms of signal to noise (S/N) and spatial definition, which clearly limits the ability to resolve temporal events accurately. The ideal imaging system would allow researchers to record calcium release events from whole cells at frame rates that would allow a more accurate determination of spark kinetics across the entire cell. Furthermore, a particularly sensitive detector is necessary not only to deliver resolvable signals at short exposure times, but also to yield low noise kinetic plots from smaller, more localized intracellular regions of interest.

We have previously reported[6] use of the world's first back-illuminated electron multiplying charge-coupled device (EMCCD) (BV-EMCCD, BV denoting optimization for visible and near IR) from Andor Technology in providing optimal signal-to-noise (S/N) performance at significantly reduced input signal levels. The EMCCD is an advanced CCD camera design, offering unsurpassed sensitivity performance, and has been shown to yield markedly improved S/N under ultra-low-light conditions *at high speed operation*, facilitating the demanding fast speed low-light microscopies such as single

Address all correspondence to Colin Coates, Andor Technology, 9 Millennium Way, Springvale Business Park, Belfast, BT12 7AL, Northern Ireland. Tel: 44-0-2890237126; Fax: 44-0-2890310792; E-mail: c.coates@andor-tech.com

1083-3668/2004/$15.00 © 2004 SPIE

molecule detection, intracellular ion signalling microscopy, and 4-D microscopy. The detector makes use of a new CCD architecture[7–12] that unites the sensitivity of an intensified CCD (ICCD), with the inherent advantages of a CCD. The EMCCD camera used in the previous preliminary study[6] contained a 128×128 pixel sensor format, currently capable of frame rates in excess of 500 fps at 10-MHz pixel readout, and was used to illustrate the combined effects of both back-illuminated sensor technology for maximum photon conversion efficiency, and EMCCD technology for eliminating the camera detection limit.

The specific effects of these technologies is to optimize the two fundamental parameters of sensitivity, detection limit, and quantum efficiency, as recapped next.[6]

- *Detection limit*. In a sufficiently cooled CCD, the detection limit is defined by the readout noise.[13] In fact, this may be regarded as the single main weakness of CCDs. Scientific CCDs can achieve 2 to 4 electrons of readout noise but only at slow readout speeds. However, at the more practical speeds of 5-MHz pixel rates or greater, this noise is typically 30 electrons or more. In applications where raw sensitivity is required, particularly at high readout rates, either intensified CCDs (ICCDs) or electron bombardment CCDs (EBCCDs) have been favored. But these detectors have their own drawbacks, such as resolution artifacts, high spurious noise, crosstalk, higher noise factor (which effectively increases the signal shot noise), and most importantly, severely restricted quantum efficiency (QE) (in the visible wavelength range) of the photocathode at the front end of light detection. They are also inherently complex and expensive devices. A more detailed comparison of these detector alternatives is given elsewhere.[11,12] Electron multiplying CCD technology, however, based on an all-solid-state design,[7–10] overcomes many of the ICCD/EBCCD drawbacks while offering amplification technology that can essentially render the readout noise negligible *at any readout speed*. That is to say, EMCCD technology (sometimes known as on-chip multiplication) affords an image sensor that is capable of detecting single photon events *without* an image intensifier, achievable by way of a unique electron multiplying structure built into the silicon, therefore avoiding the QE and resolution limitations of intensifier tubes. Gain can be increased to a degree, tuned easily through the software, where extremely weak signals may be detected above the readout noise of the camera, even under conditions of high readout noise.
- *Quantum efficiency*. Sensitivity is also dependent on QE, a measure of the light collection efficiency. In standard CCD devices, higher QE means that more incoming photons are converted to photoelectrons sufficient to overcome the noise detection limit. The higher signals afforded also reduce the relative signal shot noise. In a system such as the EMCCD, where the readout noise detection limit has essentially been removed, QE can be expected to have a direct bearing on the shot noise of the signal. Since the EMCCD does not require an intensifier tube, the full higher and broader QE curves of the CCDs can be harnessed. Indeed, even the first produced front-illuminated EMCCDs (FI-EMCCD) themselves have distinct QE advantages over ICCDs. Back-thinned CCDs, however, are recognized as having the highest QEs of any detector (up to ~95% at maximum compared to the ~45–50% maximum QE of a typical front-illuminated CCD). In terms of spectral response range the back-illuminated camera gives response from about 350 to >1000 nm, exceeding 90% over the 500- to 700-nm range. A lumogen coating can be applied to the sensor to extend response much deeper into the UV.

Therefore, the BV-EMCCD, a device that combines both electron multiplying CCD technology and back-thinned CCD technology, can be expected to offer both single photon detection sensitivity (by virtue of having eliminated the readout noise) *and* the ultimate in photon conversion efficiency (therefore improved shot noise). A back-illuminated EMCCD device can theoretically offer improvements of a factor of ×2 (or greater at some wavelengths) in signal/shot noise ratio over a front-illuminated EMCCD device. Indeed such improvements had been previously experimentally verified.[6]

This work describes some ultra-low-light experiments carried out with the iXon DV887 (BV), a back-illuminated EMCCD containing a 512×512 frame-transfer chip reading out at 10 MHz. At this readout speed, the camera can be operated at >30 fps in full frame readout, and much faster still with subarray selection or binning, as is shown. The camera has been incorporated into an ultra-low-light Nipkow spinning disk confocal microscopy arrangement for rapid calcium flux measurements on cells isolated from rabbit urethra, guinea pig bladder, and vas deferens. The results presented are instrumental in verifying three principal benefits of this technical innovation: 1. the significant influence on fundamental S/N considerations in extremely low-light cellular fluorescent microscopy scenarios; 2. the temporal/spatial resolution ability required to identify and record transient Ca^{2+} spark sites and waves; and 3. the ability of the system to record these events over long durations. In determining the improvements in sensitivity and resolution, the BV-EMCCD was directly compared (using the same cells) to the technology format that before the advent of the EMCCD camera had been considered the standard for low-light detection at fast readout speed—a GenIII+ICCD. The temporal ability was demonstrated through recording of rapid Ca^{2+} spark and wave events within the smooth muscle cells, over extended kinetic series. Sensitivity was such that kinetic profiles can be plotted of these localized events using very small region of interest (ROI) averaging, while maintaining sufficient S/N for accurate measurement.

2 Experimental Description

2.1 *EMCCD and ICCD Cameras*

The iXon DV887 (BV) from Andor Technology is a 10-MHz camera with a 512×512 frame-transfer sensor, 16-μm^2 pixel size, capable of delivering >30 full frames/sec (the precise value dependent on the vertical row shift speed selectable through the software[11]). It is important to note that much faster speeds still are achievable through selection of subarrays and/or binning. Some frame rates resulting from pixel binning and subarray combinations are given in Table 1, as-

Table 1 Frame rates (frames per second) achievable from the 10-MHz Andor iXon DV887 at a variety of subarray and binning combinations.

Array size/ binning	512×512 (full frame)	256×256	128×128	100v×512h
1×1	31	59	104	127
2×1	55.56	100	167	192
2×2	55.56	100	167	192
4×1	91.74	154	233	263
4×4	91.74	154	233	263

suming a 3.4-μs vertical shift speed. It is particularly interesting to note that 127 frames/sec is available through 100×512 subarray, without any resolution sacrifice of pixel binning. This shape of active CCD area corresponds (using a ×100 objective) to a field of view of 16×82 μm, which is sufficient to image a large proportion of typical smooth muscle cells. Recording in this mode enables such cells to be imaged at very high temporal (>100 frames/sec) and spatial resolution. Furthermore, the superior camera sensitivity is such that the S/N advantages associated with pixel binning may readily be sacrificed in favor of maintaining resolution.

The ICCD camera used was a Stanford Photonics XR Mega 10 ICCD, containing a GenIII+intensifier and 1280 ×1024 CCD sensor, 6.7-μm^2 sensor pixel size, capable of 15 frames/sec at full frame readout. The sensor is fiber coupled to the intensifier tube, with a~1.5 to 1 tapered fiber, yielding an effective pixel size of >10 μm^2. Binning (2×2) of the ICCD was necessary to enable shorter exposure times (faster frame rates) to be employed in this camera, while also making the effective pixel size more comparable to that of the EMCCD (better for more accurate sensitivity comparisons). Such binning, while imposing a sacrifice in spatial resolution, should result in more favorable S/N performance, i.e., the binned 2×2 superpixel is capable of collecting 4× as many photons as a single pixel. This ICCD is unable to perform subarray readout, so binning is the only means of increasing the frame rate.

2.2 *Intracellular Ion Measurements*

An inverted Nikon TE300 microscope with ×40 and ×100 objectives (each NA 1.3) was combined with a spinning Nipkow disk arrangement (Visitech, United Kingdom, approximately 1800 revs/min building approximately 360 complete confocal images/sec) and a krypton/argon ion laser with excitation wavelength 488 nm. A ×1.5 c-mount lens is also employed in this setup (originally inserted to compensate for the fiber taper in the ICCD). This must be taken into account during data analysis, however, when determining parameters such as ROI dimensions. Cameras were easily interchanged via a side oriented c-mount adaptor for direct comparison with the same cells under identical conditions. Freshly dispersed rabbit urethral and guinea pig cells were obtained as described previously[1] and were loaded with 10 μM of Fluo-4-AM dye (Molecular Probes, emission maximum at 516 nm) for 15 min at 37°C. Cells were plated on glass bottomed dishes, allowed to settle, and then perfused with Hanks solution maintained at 37°C. The krypton/argon ion excitation laser was sometimes varied to achieve different signal intensities, but often it was kept at standby power, i.e., the minimum power to allow stable lasing. This was considered a very desirable experimental condition, minimizing photodamage and enabling prolonged viability of the cells during continuous recording. When bound to free Ca^{2+}, the emission quantum yield of Fluo-4 increases significantly. To examine spontaneous calcium release events, cells were deliberately chosen that have been demonstrated to fire Ca^{2+} sparks[3] and Ca^{2+} waves.[4] Occasionally, caffeine addition (10 mM for 5 sec) was used to induce release of intracellular Ca^{2+} from the cellular calcium stores and resulted in a rapid build up (more than tens of milliseconds) of Ca^{2+} levels within the cell, followed by a slower (hundreds of milliseconds—seconds) decay of the intracellular Ca^{2+} concentration. Calcium flux dynamics were readily analyzed and displayed using quantitative processing functions with Andor's imaging software. During analysis, region of interest (ROI) boxes are employed, selectable from within the Andor imaging software, from which average values may be calculated from the pixels contained within. To smooth the images, a standardized smoothing algorithm from NIH Image was applied to the raw images. This algorithm is based on a nearest-neighbor averaging method that creates a value for each pixel based on the average calculated for that pixel and its surrounding eight pixels.

3 Results and Discussion

To perform a direct performance comparison between the BV-EMCCD camera and the Gen III+ICCD, a series of Fluo-4 loaded rabbit urethra smooth muscle cells were imaged, taking a short kinetic series (10 frames) with one camera, then performing the same analysis with the other camera directly after with the same cell still in place. The order in which the images were recorded was alternated for each subsequent cell, to rule out photobleaching effects on the differing S/N levels. In general, largely due to the rapid confocal nature of the technique and the short 33-ms exposure times employed (2×2 binning of the ICCD was necessary to achieve this exposure), the fluorescent images represent extremely low photon fluxes. All cells imaged were within the same field of cells and subjected to identical dye loading times. However, it was obvious that some cells were inherently weaker than others. This is due to slightly different loading efficiencies, focal fine position, and also, the laser power was purposefully varied slightly to produce different degrees of signal intensities. The important point was that each cell was imaged like-for-like, varying only the camera.

Figure 1(a) shows one of the cells recorded with each camera type, both before and after applying a smoothing algorithm. It is clear that both signal contrast and resolution are markedly better in the case of the images recorded with the BV-EMCCD. The effect of smoothing is to enhance the contrast further between fluorescent signal and background, at the expense of some resolution. However, even after smoothing of each image, the same improvements are noticeable in the BV-EMCCD images compared to the corresponding ICCD

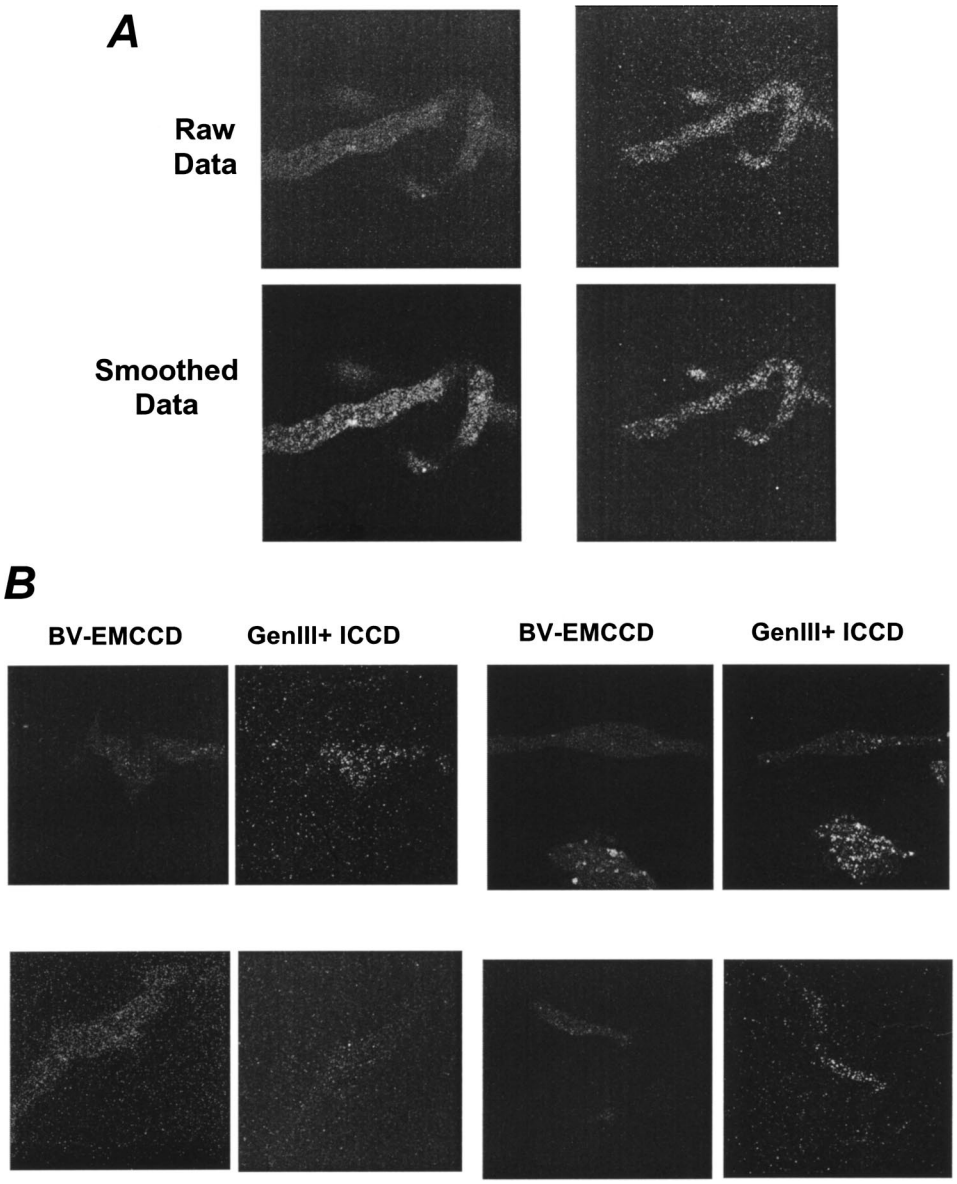

Fig. 1 (a) Comparative raw and smoothed low-light fluorescent images recorded from a live smooth muscle cell using the BV-EMCCD and the Gen III+ICCD. (b) Further smoothed images recorded of Fluo-4 loaded smooth muscle cells using both the BV-EMCCD and the Gen III+ICCD; 33-ms exposure time per frame; high EM or ICCD gain setting throughout.

image. Figure 1(b) shows a representative series of comparative cell images from this experiment, each having been smoothed to provide clearer visualization, particularly of the ultra-weak images. It is clear that signal intensity and image contrast were better throughout the series for the images recorded with the EMCCD, a direct function of a higher S/N ratio afforded by the higher QE of the EMCCD detector (both types of detector have overcome the read noise detection limit). This pattern has been observed previously for the iXon DV860, 128×128 sensor, versus the same Gen III+ICCD, albeit across a series of different cells within the same field.[6] The degree of improvement is particularly apparent for cell 3, for which the photon flux was so low that it could barely be detected at all with the ICCD, but is certainly identifiable with the EMCCD. The superior signal of the EMCCD is to be expected, given the markedly restricted QE of ICCDs compared to the unrestrained QE of the BV-EMCCD. Indeed, at the 516-nm λ_{max} of Fluo-4 dye, the BV-CCD should have $>\times 2$ QE than a GenIII+photocathode. This should result in $>\times 1.4$ increase in signal-to-shot noise ratio.

Furthermore, the resolution from the BV-EMCCD is markedly better, and one can more easily identify areas of intracellular dye compartmentalization, for example. This resolution improvement arises to a large extent from the different electron amplification technology used in the EMCCD, which virtually eliminates the pixel cross talk that is inherent in ICCD measurements (yielding a form of instrumental blurring),[12] but also from the slightly larger area of the 2×2 binned pixel required to run at a faster readout speed (and shorter exposure time). In comparison, the EMCCD produces images of stark resolution—postacquisition smoothing can be applied artificially through software if required, but this is the

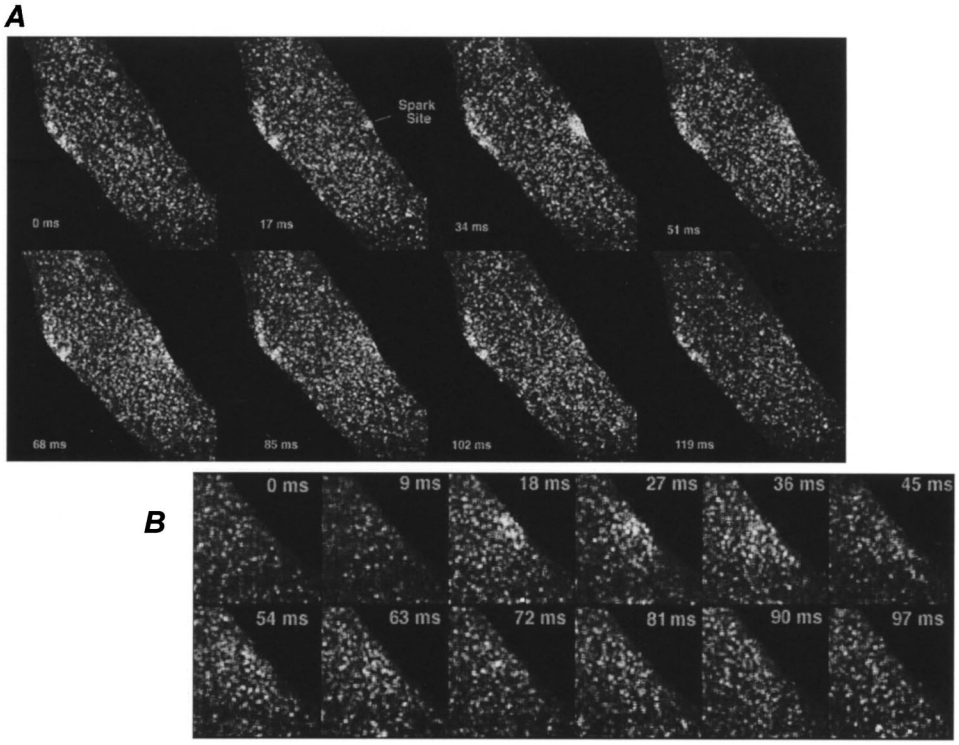

Fig. 2 (a) Consecutive BV-EMCCD fluorescence images from a 1500-frame kinetic series at 59 frames/sec, 256×256 subarray, showing the initiation and spread of a single Ca^{2+} spark. (b) Consecutive images from the same cell at 113 frames/sec, 100×100 subarray. The cell section is shown against the black background, from which no fluorescence is observed.

researcher's choice. It is interesting also to note that, in terms of sensitivity, a greater number of photons should hit the slightly larger pixel area of the 2×2 binned ICCD than that of the nonbinned BV-EMCCD, yet the latter camera clearly maintained a clear S/N advantage (without the need to sacrifice resolution for speed).

It is important to note that all of the images shown here are of extremely weak signals, and would be lost entirely within the read noise floor if it were not for the respective signal amplification technologies.

To provide a better depiction of the temporal capabilities of this latest 10-MHz BV-EMCCD camera, a series of cells were chosen from which fast Ca^{2+} sparking events could be imaged in extended kinetic series, either with full frame or subarea (the latter can be tailored to achieve both faster speeds and to match the dimensions of the muscle cells). The events either occurred naturally within the cell or were induced through controlled injection of caffeine to stimulate Ca^{2+} release. Generally, it is highly desirable to record as many images as possible within the duration of a sparking event or wave, such that a clear spatial and temporal profile of the intracellular calcium activity can be generated. In fact, one approach that is currently used to get maximum temporal resolution is to employ a line scanning technique.[5] To obtain such high temporal resolution (500 frames/sec), a significant sacrifice in spatial resolution is required (i.e., the scanned region is only 1 pixel diam).

Figure 2(a) shows a series of selected images from a 1100-frame kinetic series recorded of Fluo-4 loaded guinea pig bladder smooth muscle cell with the BV-EMCCD, operated with 256×256 pixel subarray at 59 frames/sec. The montage of consecutive images represent a Ca^{2+} spark event, which can be seen to rapidly appear close to the cell membrane and spread into the cell. A smaller 100×100 pixel subarray was then placed on top of the sparking region of this cell, such that a frame rate of 113 frames/sec was obtainable from a more targeted field of view. This function is readily achievable from within the Andor imaging software, requiring the customizable subarray box simply to be dragged on top of the interesting region. Figure 2(b) shows a montage of consecutive images derived from one of the sparking events at this faster frame rate, from which the dynamics of the event occurring within this field of view can be more readily discerned.

Kinetic plots, shown in Fig. 3, were generated from a ROI function within the Andor software, from a 2.7-μm ROI over the spark site shown in Figs. 2(a) and 2(b), therefore showing comparative kinetics at 59 and 113 frames/sec. In all cases, the Ca^{2+} spark events are clearly recognizable above the basal fluorescence level. Figures 3(b) and 3(d) show one of the spark profiles from each series expanded out to give a clearer depiction of the number of data points present within a given event, each data point derived from a single image capture. It is clear from this figure that differences in activation and decay kinetics of the spark are clearly identifiable.[2] The corresponding 113 frames/sec kinetic plot shown in Fig. 3(d) clearly shows more data points per event. To highlight this comparison further, Fig. 3(e) shows expanded kinetic profiles, plotted as a function of frame number, at 59 frames/sec (from Fig. 2) and 113 frames/sec. The spark events are clearly more temporally defined at the faster speeds, yet maintain sufficient

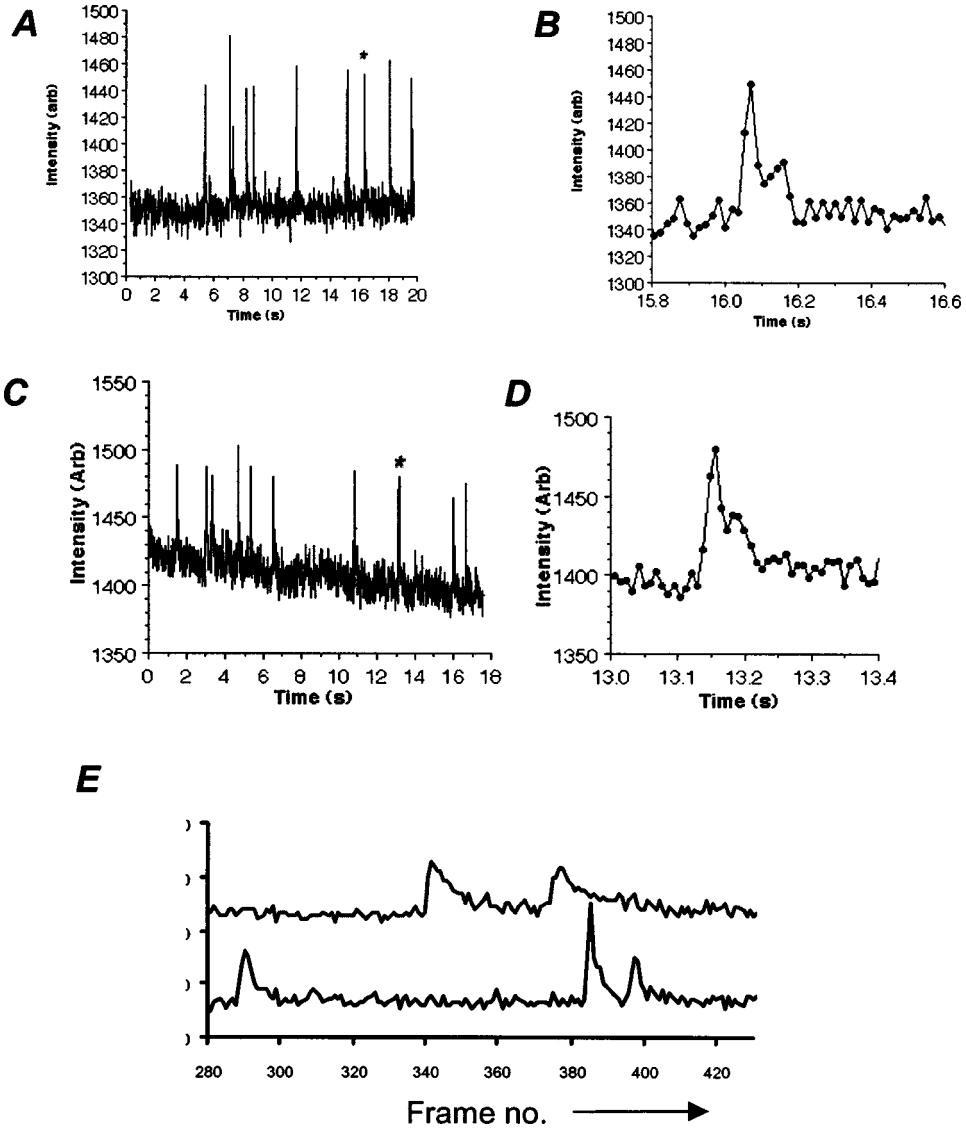

Fig. 3 Kinetic plots derived from ROI averages of the 1100-frame kinetic series of Fig. 2: (a) 59 frames/sec; (b) 59 frames/sec expanded spark of the asterix event in (a); (c) 113 frames/sec; (d) 113 frames/sec expanded spark (the baseline slope is due to an offset artifact that has since been rectified); and (e) 59 and 133 frames/sec expanded and overlaid.

S/N despite the shorter exposure times employed. This ability to go to higher temporal resolution while maintaining the sensitivity to deal with the lower signal levels associated with shorter experiments is highly desirable for recording such Ca^{2+} spark events.

The ability of this system to record calcium release events at high temporal resolution is further demonstrated in Fig. 4. In this experiment, the effects of applying caffeine (10 mM) were examined on a quiescent smooth muscle cell. Figure 4(a) shows a montage of images selected from a 1100-frame kinetic series, at 60 frames/sec, of a Fluo-4 loaded bladder smooth muscle cell, during which caffeine was added to induce a Ca^{2+} release from ryanodine sensitive stores. As the fourth panel of Fig. 4(a) demonstrates, it was possible to observe the initial site of Ca^{2+} release, which then spread across the entire cell (subsequent images). Figure 4(b) shows kinetic plots recorded from two regions of interest, one at the point of Ca^{2+} release and one close to the extremity of the cell [bottom of the cell as viewed in Fig. 4(a)]. By using such an analysis, one can build up a clear profile of the response, decay, and magnitude of the wave event, and can also measure the time taken to spread across the cell. Without a camera of sufficient sensitivity as well as temporal and spatial resolution, rapidly spreading events such as this would be very difficult to characterize in terms of both confidently identifying the localized region of weak initial activity, and recording this initiation with sufficient data points.

Recently Sergeant et al.[1] demonstrated the presence of spontaneous transient inward currents in specialized pacemaking cells in the rabbit urethra, and later suggested that these may be due to formation of a spontaneous Ca^{2+} wave in these cells.[4] To test this idea and to demonstrate that continuous recording of these events was possible over a long duration, we examined activity in an isolated interstitial cell from the rabbit urethra loaded with Fluo-4-AM. Figure 5(a) shows a selection of images taken from a 1500 kinetic series of images

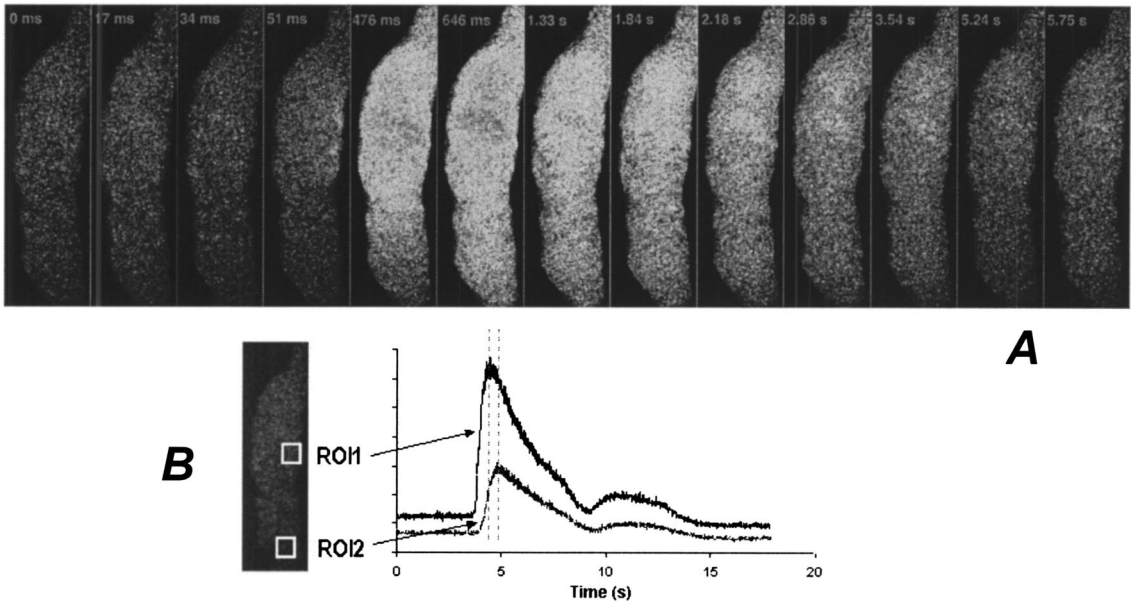

Fig. 4 (a) Selected fluorescence images from a 1100-frame kinetic series at 60 frames/sec, showing the progression of a caffeine-induced Ca^{2+} transient event in guinea pig bladder myocyte. (b) Kinetic plots derived from offset ROIs within the cell.

acquired at 30 frames/sec. It is clear from these images that Ca^{2+} oscillations arise from one region of the cell and are propagated throughout the cell. To analyze the spread of this wave throughout the cell, two 50×50-pixel ROIs were placed at opposite ends of the cell. The resultant plots, shown in Fig. 5(b), clearly show an overlaid series of offset wave events, the peaks arising from the bottom ROI appearing consistently ahead of those from the top ROI, from which the transverse

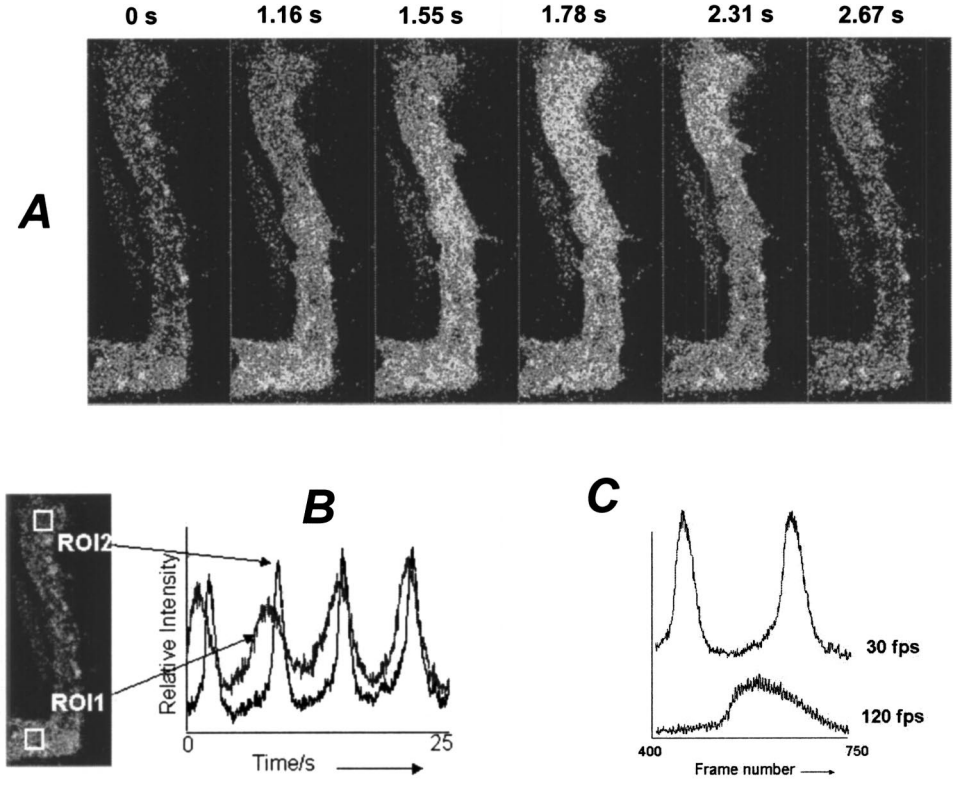

Fig. 5 (a) Selected fluorescence images from a 1500-frame kinetic series at 30 frames/sec, showing the progression of a Ca^{2+} wave as it progresses though a rabbit urethral cell. (b) Kinetic plots derived from offset ROIs within the cell. (c) Comparison of kinetic plots generated from 30 and 120 frames/sec kinetic series of the same cell (the 120 frame/sec images used the same field of view, varying only the exposure time).

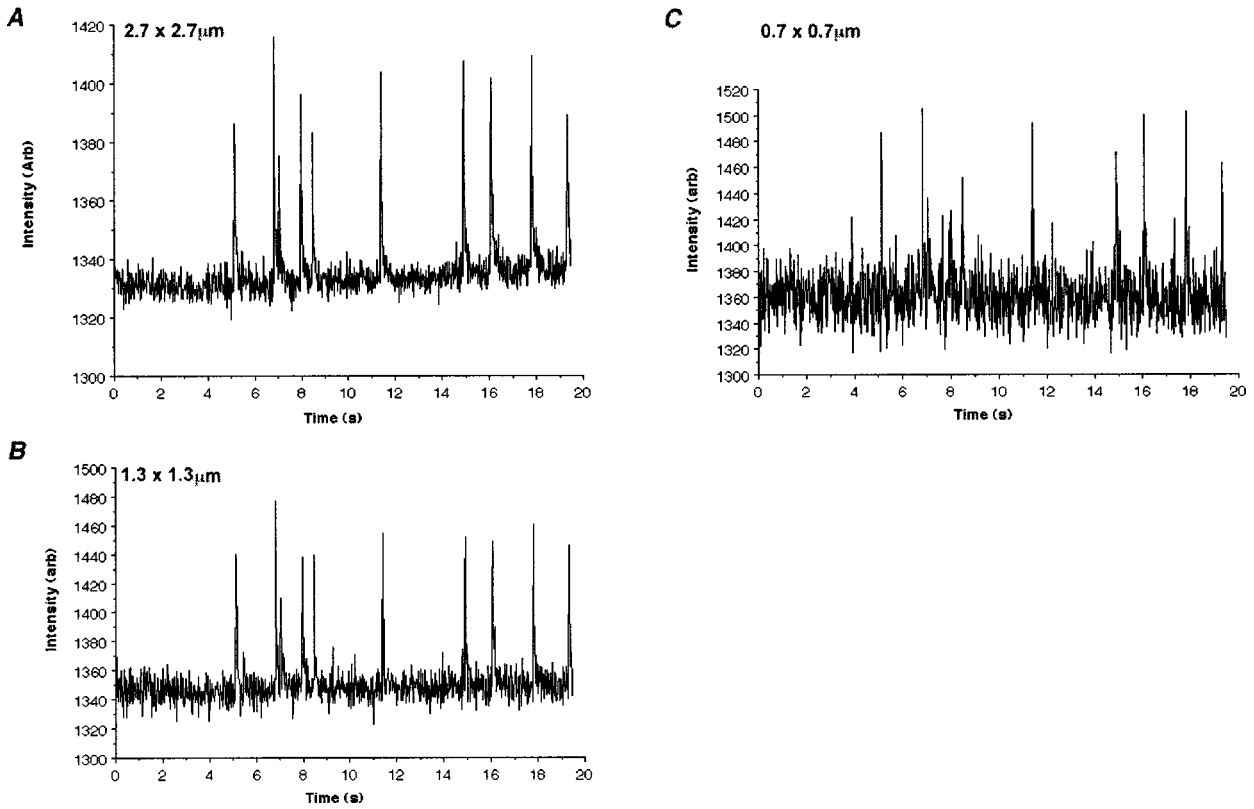

Fig. 6 Kinetic plots generated from ROIs of different sizes, 2.7, 1.3, and 0.7 μm^2; the ROIs placed within the cell spark site analyzed in Figs. 2 and 3.

time of the wave is measurable. It is interesting to note that the delay between the peaks varies slightly from wave to wave and that, in contrast to the guinea pig smooth muscle, no distinct spark-like events could be detected. To illustrate the ability to measure these events at faster speeds, kinetic series were recorded at 60 and 120 frames/sec also. Figure 5(c) shows a section of the ROI kinetic plot obtained at 30 frames/sec, compared to a wave recorded at 120 frames/sec. While it is clear that the progressively shorter exposure times employed to afford greater temporal resolution resulted in a lower S/N ratio, the camera's ultra-sensitive performance was such that even at 120 frames/sec, the Ca^{2+} wave profile could still be clearly discerned. It is important to note that the subarray used to give 120 frames/sec was sufficient to image the entire cell at this speed without need for pixel binning.

During analysis, ROIs are employed, selectable from within the Andor imaging software, from which average values may be calculated from the pixels contained within. If small ROIs are used, this feature may allow researchers to examine events that are spatially smaller than sparks, i.e., Ca^{2+} quarks.[14] Figure 6 shows a series of kinetic profiles generated from the studied spark site of the 59 frames/sec kinetic series of images examined in Fig. 2. The profiles were generated from three different sizes of ROI placed at the center of the sparking region, which when the ×100 objective and ×1.5 c-mount lens are accounted for, correspond to ROIs of ~2.7×2.7 μm^2, 1.3×1.3 μm^2, and 0.7×0.7 μm^2. It is clear that the S/N ratio decreases as the ROI area decreases, as expected. However, camera sensitivity is such that the sparks can be confidently identified, even from the smallest ROI area.

4 Conclusions

The significant boost in ultra-sensitive imaging performance offered by the new back-illuminated EMCCD is demonstrated here in the context of measured improvements to a particularly demanding ultra-low-light microscopy technique. Improvements are in the form of sensitivity, resolution, and speed parameters that are to a large extent interdependent. This enhanced sensitivity offered by this camera complements its ability to deal with the lower photon fluxes associated with the shorter exposure times inherent to fast frame rate operation. Furthermore, through intelligent choice of subarray selection, very fast frame rates (>100 frames sec) are achievable without sacrifices to pixel resolution. The higher sensitivity will also prove entirely useful in enabling use of both lower fluorophore concentrations, lower excitation powers, higher optical magnifications and smaller ROI analysis, conditions employed for the most part in the current study. The BV-EMCCD will undoubtedly be used in the optimization of a number of challenging low-light microscopy approaches (and indeed low-light macroscopic approaches also), including single molecule microscopy[15,16] and 4- or 5-D live cell microscopy.

Acknowledgments

Authors McHale, Thornbury, and Hollywood wish to acknowledge financial support from the Wellcome Trust, Action Medical Research, and the Medical Research Council.

References

1. G. P. Sergeant, M. A. Hollywood, K. D. McCloskey, K. D. Thornbury, and N. G. McHale, ''Specialised pacemaking cells in the rabbit urethra,'' *J. Physiol. (London)* **526**, 359–366 (2000).
2. J. H. Jaggar, V. A. Porter, W. J. Lederer, and M. T. Nelson, ''Calcium sparks in smooth muscle,'' *Am. J. Physiol.* **278**, 235–56 (2000).
3. G. M. Herrera, T. J. Heppner, and M. T. Nelson, ''Voltage dependence of the coupling of Ca(2+) sparks to BK(Ca) channels in urinary bladder smooth muscle,'' *Am. J. Physiol.* **280**, 481–90 (2001).
4. M. A. Hollywood, L. Johnston, N. G. McHale, and K. D. Thornbury, ''Spontaneous calcium transients in isolated interstitial cells from the rabbit urethra,'' *J. Physiol. (London)* **548P**, 16 (2003).
5. C. White and J. G. McGeown, ''Inositol 1,4,5-trisphosphate receptors modulate Ca2+ sparks and Ca2+ store content in vas deferens myocytes,'' *Am. J. Physiol.* **285**, C195–C204 (2003).
6. C. G. Coates, D. J. Denvir, E. Conroy, N. McHale, K. Thornbury, and M. Hollywood, ''Back-illumintated electron multiplying technology; The world's most sensitive CCD for ultra low-light microscopy,'' see http://www.emccd.com/papers.htm.
7. P. Jerram et al., ''The LLLCCD: Low light imaging without the need for an intensifier,'' *Proc. SPIE* **4306**, 178–186 (2001).
8. C. D. Mackay et al., ''Sub-electron read noise at MHz pixel rates,'' see http://www.marconitech.com/ccds/13vision/technology.php.
9. S. H. Spencer and N. J. Catlett, ''Low light level solid state TV imaging,'' see http://www.marconitech.com/ccds/13vision/technology.php (Mar. 2000).
10. E. J. Harris et al., ''Evaluation of a novel CCD camera for dose reduction in digital radiography,'' see http://www.marconitech.com/ccds/13vision/technology.php.
11. D. J. Denvir and C. G. Coates, ''Electron multiplying CCD technology: Application to ultrasensitive detection of biomolecules,'' *Proc. SPIE* **4626**, 502–512 (Jan. 2002).
12. D. J. Denvir and E. Conroy, ''Electron multiplying CCD technology: The new ICCD,'' *Proc. SPIE* **4796**, 164–174 (2002).
13. J. R. Janesick, *Scientific Charge-Coupled Devices*, SPIE Press, Bellingham, WA (2001).
14. E. Niggli, ''Localized intracellular calcium signalling in muscle: Calcium sparks and calcium quarks,'' *Annu. Rev. Physiol.* **61**, 311–335 (1999).
15. R. M. Dickson et al., ''On/off blinking and switching behaviour of single molecules of green fluorescent protein,'' *Nature (London)* **388**, 355–358 (1997).
16. T. A. Byassee, W. C. W. Chan, and S. Nie, ''Probing single molecules in single living cells,'' *Anal. Chem.* **72**, 5606–5611 (2000).